7

# Freshwater Dispersion Plume in the Sea: Dynamic Description and Case Study

Renata Archetti and Maurizio Mancini
*DICAM University of Bologna, Bologna*
*Italy*

## 1. Introduction

An interesting mesoscale feature of continental and shelf sea is the plumes produced by the continuous discharge of fresh water from a coastal buoyancy source (rivers, estuarine or channel).
The general spreading of freshwater plume depends on a large number of factors: tide, out flowing discharge, wind, local bathymetry, Coriolis acceleration, inlet width and depth.
The discharge of freshwater from coastal sources drives an important coastal dynamic, with significant gradients of salinity. These phenomena are highly dynamic and have several effects on the coastal zone, such as reducing salinity, changing continuously the vertical profiles and distribution of parameters, such as dissolved matters, pollutants and nutrients (Jouanneau & Latouche, 1982; Fichez et al., 1992; Grimes & Kingford, 1996; Duran et al., 2002; Froidefond et al., 1998; Broche et al., 1998; Mestres et al., 2003; Mestres et al., 2007).
As a result of these effects, several classification schemes based on simple plume properties have been proposed in an attempt to predict the overall shape and scale of plumes. Kourafalou et al. (1996) classified plumes as supercritical and subcritical, according to the ratio between the outflow and the shear velocity. Yankovsky and Chapman (1997) derived two length scales based on outflow properties (velocity, depth and density anomaly) and used them to discriminate between bottom-advected, intermediate and surface-advected plumes, depending on the vertical and horizontal density gradients near the plume front; in spite of the absence of external forcing mechanisms in their theory, they correctly predicted the plume type for several numerical and real cases. Garvine (1987) classified plumes as supercritical or subcritical using the ratio of horizontal discharge velocity to internal wave phase speed and he later proposed (Garvine, 1995) a classification system based on bulk properties of the buoyant discharge.
Referenced plume studies present numerical modelling of the case, in situ observations (Sherwin et al., 1997; Warrick & Stevens, 2011; Ogston et al., 2000), satellite observations (Di Giacomo et al., 2004; Nezlin and Di Giacomo, 2005; Molleri et al., 2010) or aerial photographs (Figueiredo da Silva et al., 2002; Burrage et al., 2008). In several cases two techniques are coupled (O'Donnell, 1990; Stumpf et al., 1993; Froidefond et al., 1998; Siegel et al., 1999).
In this work a freshwater dispersion by a canal harbour into open sea is described in depth with the aim of a 3D numerical model and with the validation of in situ measurements carried out with innovative instruments. The measurements appear in literature for the first

time. The investigated area relates to the coastal zone near Cesenatico (Adriatic Sea, Italy). The aim of this chapter is to describe the dynamic of freshwater dispersion and to show the results of the simulation of flushing, mixing and dispersion of discharged freshwater from the harbour channel mouth under different forcing conditions.
The chapter will be organized in the following sections:

- Introduction with focus on research and works dealing with the modelling of freshwater dispersion plumes in the sea and their comparison with existing data;
- Description of the numerical model;
- Physical features of the case study;
- Plume modelling on Cesenatico (Italy) discharging area;
- Validation of model results with in situ measurement campaigns;
- Conclusions.

## 2. The numerical model

The numerical model is based on motion and continuity equations (Liu & Leendertse, 1978) tested by the authors. The model utilizes a Liu and Leendertse's scheme describing vertical water motion by calculation of the turbulence field. The model equations for conservation of momentum and continuity, written in Cartesian coordinates, in incompressible fluid conditions and under the effects of Earth's rotation are:

$$\frac{\partial u}{\partial t}+\frac{\partial (uu)}{\partial x}+\frac{\partial (uv)}{\partial y}+\frac{\partial (uw)}{\partial z}-f\cdot v+\frac{1}{\rho}\frac{\partial p}{\partial x}-\frac{1}{\rho}\left(\frac{\partial \sigma_x}{\partial x}+\frac{\partial \tau_{xy}}{\partial y}+\frac{\partial \tau_{xz}}{\partial z}\right)=0 \tag{1}$$

$$\sigma_x = A_x\frac{\partial u}{\partial x};\qquad \tau_{xy}=A_x\frac{\partial u}{\partial y} \tag{2}$$

$$\frac{\partial v}{\partial t}+\frac{\partial (vu)}{\partial x}+\frac{\partial (vv)}{\partial y}+\frac{\partial (vw)}{\partial z}+f\cdot u+\frac{1}{\rho}\frac{\partial p}{\partial y}-\frac{1}{\rho}\left(\frac{\partial \tau_{yx}}{\partial x}+\frac{\partial \sigma_y}{\partial y}+\frac{\partial \tau_{yz}}{\partial z}\right)=0 \tag{3}$$

$$\sigma_y = A_y\frac{\partial v}{\partial y};\qquad \tau_{yx}=A_y\frac{\partial v}{\partial y} \tag{4}$$

$$\frac{\partial w}{\partial t}+\frac{\partial (wu)}{\partial x}+\frac{\partial (wv)}{\partial y}+\frac{\partial (ww)}{\partial z}+\frac{1}{\rho}\frac{\partial p}{\partial z}-\frac{1}{\rho}\left(\frac{\partial \tau_{zx}}{\partial x}+\frac{\partial \tau_{zy}}{\partial y}+\frac{\partial \sigma_z}{\partial z}\right)+g=0 \tag{5}$$

$$\frac{\partial u}{\partial x}+\frac{\partial v}{dy}+\frac{\partial w}{dz}=0 \tag{6}$$

where $t$ denotes time, x, y and $z$ are Cartesian coordinates (positive towards Est, South, up) $u$, $v$, $w$ denote velocity components in the direction of $x$, y, z, $f$ is the Coriolis parameter (assumed to be a constant), $g$ is the acceleration due to gravity, ρ is the density of water, $A$ is the horizontal eddy viscosity $\sigma_i$, $\tau_{ij}$ with i, j = x, y, z components of Reynolds tensor proportional to vertical gradient of velocity. In accordance with other authors it was assumed as adequate the use of two-dimensional depth-integrated equations for

conservation of mass and momentum for a typically well-mixed water column due to wind and tidal stirring. So the vertical momentum equation has been substituted by baroclinic pressure equation (8) where sea water density has been formulated according with the international thermodynamic equation of sea water based on the empirical state function of UNESCO81 which links density to Salinity, Temperature and Pressure:

$$\frac{\partial S}{\partial t}+\frac{\partial (Su)}{\partial x}+\frac{\partial (Sv)}{\partial y}+\frac{\partial (Sw)}{\partial z}-\frac{\partial}{\partial x}\left[D_x\frac{\partial S}{\partial x}\right]-\frac{\partial}{\partial y}\left[D_y\frac{\partial S}{\partial y}\right]-\frac{\partial}{\partial z}\left[k\frac{\partial S}{\partial z}\right]=0 \tag{7}$$

$$\frac{\partial p}{\partial z}+\rho(S,T)g=0 \tag{8}$$

$$\frac{\partial T}{\partial t}+\frac{\partial (Tu)}{\partial x}+\frac{\partial (Tv)}{\partial y}+\frac{\partial (Tw)}{\partial z}-\frac{\partial}{\partial x}\left[D_x\frac{\partial T}{\partial x}\right]-\frac{\partial}{\partial y}\left[D_y\frac{\partial T}{\partial y}\right]-\frac{\partial}{\partial z}\left[k^1\frac{\partial T}{\partial z}\right]=0 \tag{9}$$

*S* and T are salinity and temperature, respectively. $D_x$ ,$D_Y$ are horizontal eddy diffusivities for *S* and T; k and k′ are vertical diffusion coefficients for mass and wheat. For vertical balance an E coefficient of vertical exchange is introduced for momentum which relates vertical Reynolds forces to the vertical gradient of horizontal components of velocities and expressed by Kolmogorov e Prandtl as:

$$E=\rho L\sqrt{e}\exp^{(-mRi)} \tag{10}$$

$$Ri=-\frac{g}{\rho e}\frac{\partial \rho}{\partial z}L^2 \tag{11}$$

$$L=\chi z\sqrt{1-\frac{z}{d}} \tag{12}$$

$$\tau_{xz}=E_x\frac{\partial u}{\partial z} \tag{13}$$

$$\tau_{yz}=E_y\frac{\partial v}{\partial z} \tag{14}$$

where m is a numeric parameter and *Ri* is the Richardson number in terms of vertical gradient of density (ρ) and of eddy kinetic energy (e) and L defined, according with Von Kàrman, by $\chi$ (numerical coefficient) and d distance of bottom (z=0) from surface (z=d). Vertical exchange coefficients for mass (k) and heat (k′) are defined similarly to E coefficients using adequate parameters substitutive of ρ and m. The adopted vertical scheme introduces eddy kinetic energy as a state function which requires its own dynamic equation for balance and conservation:

$$\frac{\partial e}{\partial t}+\frac{\partial (eu)}{\partial x}+\frac{\partial (ev)}{\partial y}+\frac{\partial (ew)}{\partial z}-\frac{\partial}{\partial x}\left[D_x\frac{\partial e}{\partial x}\right]-\frac{\partial}{\partial y}\left[D_y\frac{\partial e}{\partial y}\right]-\frac{\partial}{\partial z}\left[E_e\frac{\partial e}{\partial z}\right]+S-D_e=0 \tag{15}$$

with horizontal and vertical exchange eddy diffusivities $D_x$ $D_y$ and $E_e$ were defined in a similar way to exchange mass coefficients. So energy sourcing into the grid is detected in the function of strain tensions induced by vertical velocity and the term of energy dissipated by shear stress at the bottom is calculated from energy in flux direction in lower level S and Chézy shear coefficient C. In the surface layer a wind effect generating turbulence by waves is considered in the higher part of the water column. Supposing constant motion for the sea, *Et* is the total energy generated for surface units in the function of wind velocity

$$S = L\sqrt{e}\left(\frac{\partial \bar{u}}{\partial z}\right)^2 \tag{16}$$

$$D_e = a_2 \frac{e^{3/2}}{L} \tag{17}$$

$$S = g\frac{U^3}{C^2} \tag{18}$$

$$E_t = 5.610^{-9} u_w^4 \tag{19}$$

where $u$ is the mean velocity, $D_e$ the dissipation coefficient, $a_2$ a constant parameter taking account of energy transfer from high to small turbulence conditions and $uw$ the wind velocity.
The model equations are discretized and solved into a finite-difference formulation.

## 3. Physical features of the case study

The study site of the present survey is the pulmonary system of Cesenatico canal harbour (Northern Adriatic Sea, Italy) and the near coastal zone (Mancini, 2009). An aerial view of the canal harbour in Cesenatico is shown in Fig. 1A. During summer and in dry weather conditions the main part of discharged freshwater comes from waste water treatment plants (WWTP) and from drainage pipe systems. Treated and untreated wastewaters reach the canal with high hourly variations and the sea outlet provides regulated discharge into sea according to unsteady tidal flow. Generally the harbour canal, having a very low ground slope, guarantees a good thermoaline turbulent mixing, for the entire water column, if the basin structure presents a high pulmonary surface/wastewater loading ratio. Small estuaries with higher ground slope, receiving sea water by tidal oscillations within a few hundred metres from the coast-line and high flow rate coming from WWTP, present flow primarily directed to the sea where freshwater continuously flows on the surface. Cesenatico canal harbour basin reveals a condition where the pulmonary area and freshwater input from inland (300.000 EI, Equivalent Inhabitants) produce in the canal mouth vertical profiles of velocity, turbulent thermoaline mixing and depth of the overflowing layer daily and hourly varying in function of tidal type and phase (Bragadin et al., 2009). The investigated area is characterized by a low constant slope of the bottom and starts from the canal harbour mouth towards to a 2000 m radius. The near coastal zone is characterized by submerged breakwaters in a northerly direction and by emerged breakwaters in a southerly direction. The discharging plume area and its vertical profiles of

thermoaline and quality parameters appear strongly conditioned by external waves and currents also in dry weather conditions. Recent monitoring investigations (Mancini, 2009) reveal vertical parameter profiles at mouth varying from an initial uniform vertical profile, also in correspondence with low tidal outgoing ranges. During these conditions, reinforced afternoon wind generates significant sea waves, which oppose the surface freshwater flow. On the contrary, during nightly major outgoing tidal phases, strong stratification is maintained in the mouth zone, as in the dispersion plume area facing the breakwaters. Morphologic, hydraulic and water quality measurements have been executed into the transition estuary of the harbour canal and near the mouth of adjacent breakwaters (a view of the breakwater is shown in Fig. 2B).


A

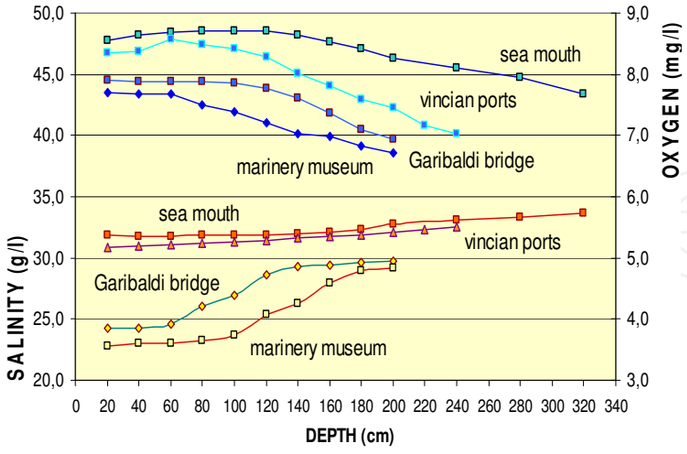


B

Fig. 1. A) Aerial view of Cesenatico. The bullets represent the position of the sample in Fig. 1B: from the city centre to the sea, respectively: Mariner Museum, Garibaldi Bridge, Vincian Ports and sea mouth. B) Salinity and oxygen profiles inside the harbour canal in the position plotted in nearby Fig. 1A.

Other research activities, carried out on freshwater-sea water balance for the volumes of channels of the Cesenatico Port Canal system, (Mancini, 2008) indicated that wastewater, discharged in the internal zone, has a hydraulic retention time before sea dispersion, ranging between 1 and 3 days. As a consequence, there is a freshwater storage in the most internal parts of the channel during incoming tidal phases; on the other side during the outgoing tidal phases, there is the outflow of the main part of the internal storage freshwater. Fig. 2B shows monitoring data in correspondence with an internal channel section at 4 Km from the mouth. The selected section balance between saline waters introduced by tidal oscillations combined with wastewater flux incoming from inland maintains the salinity range within a 0-3 g/l. The figure also plots oxygen and redox, showing similar behaviour.

A

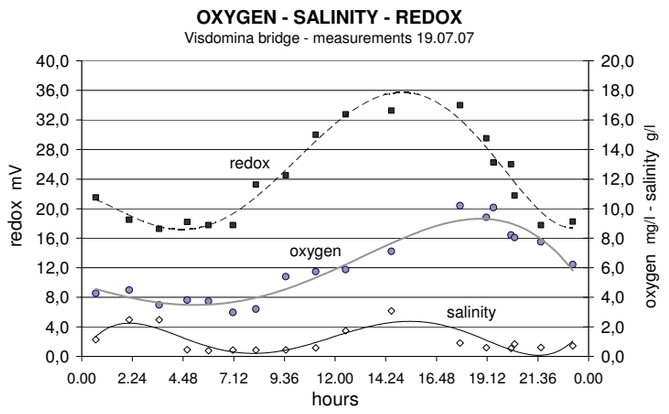


B

Fig. 2. A) Cesenatico northern coastal area characterized by submerged breakwaters. B) Daily behaviour of physical-chemical parameters measured in the internal section of the channel limiting transition volumes.

Before the outfall these outgoing volumes flow through the historical tract of the harbour which presents depths varying between 3 to 5 m. In this tract a typical overflowing volume upon the static higher density deep layers (Fig. 1B) can be observed. The Marinery Museum

and Garibaldi Bridge are located in the canal, approx. 500 m from the mouth, the Vincian Ports are located 50 m from the sea mouth. In the last tract close to the mouth a partial mixing with sea water is permitted, that increases salinity, oxygen and pH, according to the external sea conditions.

## 4. Plume modelling on Cesenatico (Italy) discharging area

The hydrodynamic model described above has been used to simulate the evolution of the plume originating from the freshwater discharge from the harbour canal. The bathymetry and the geometry of the breakwaters and structures were modelled by a small mesh dimension. The regular mesh, shown in Fig. 3, was made by 144x170 grid points, with cell dimensions 12 m x 12 m. On the same figure it is possible to recognize the shoreline, the harbour canal (points P2, P3 and P4) and coastal defence structures, parallel to the shoreline. The points on the same Fig. 3 are the profile points where measurements, later described, have been carried out.

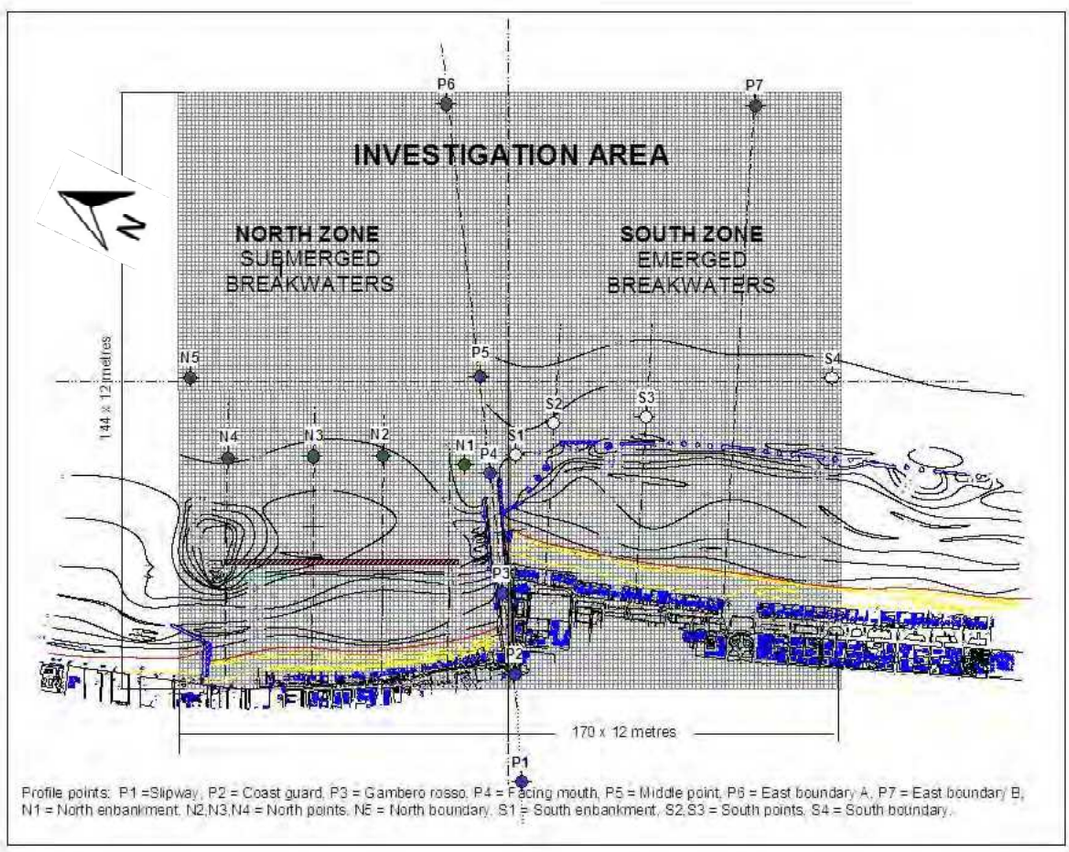


Fig. 3. Investigation area, calculation mesh utilized in model simulations and location of the fixed investigated points.

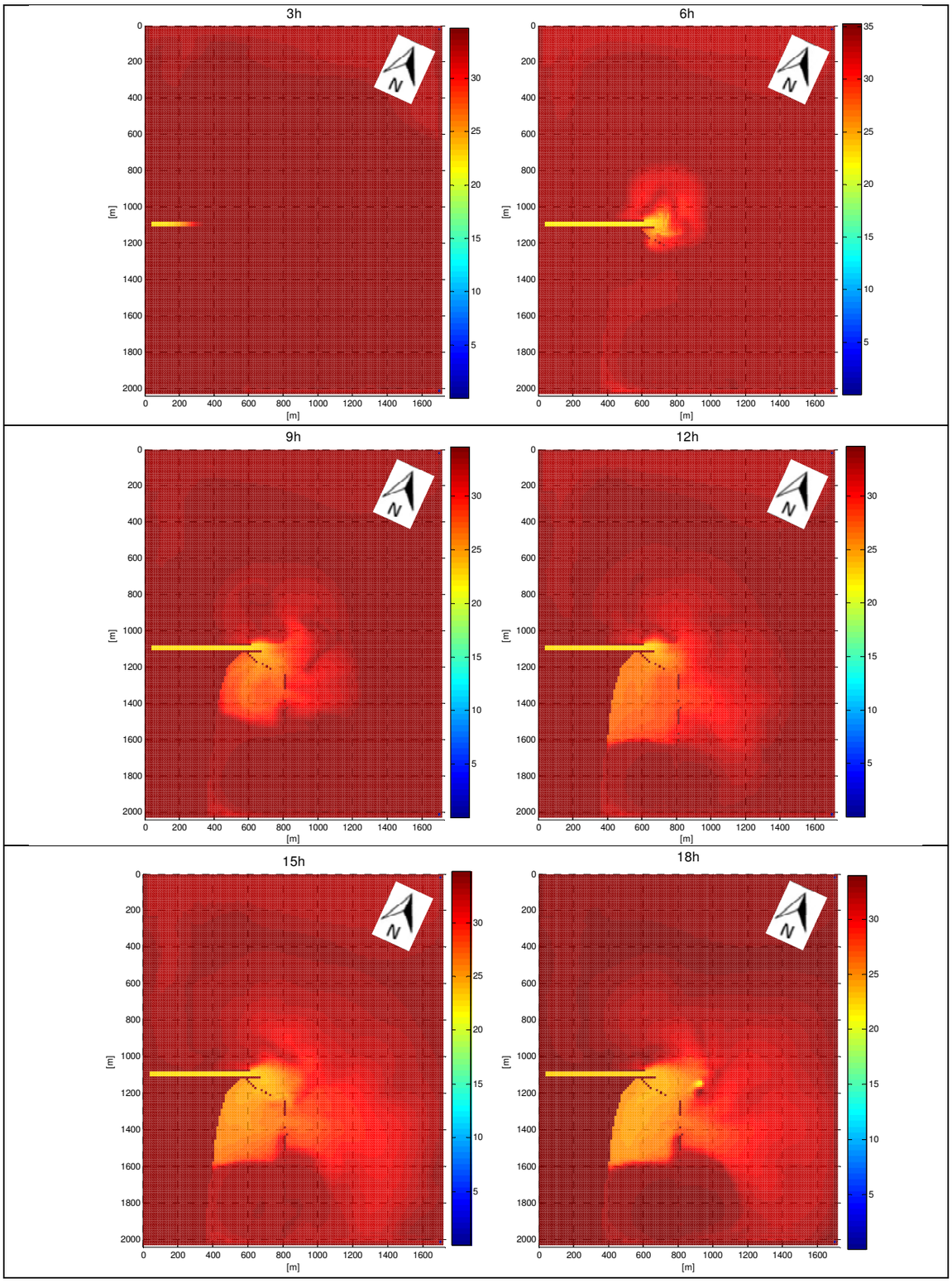


Fig. 4A. Example of simulation results of the freshwater plume dispersion in different tidal phases plotted in Fig. 4B.

A typical summer condition is shown in Fig. 4, the hydrodynamic and dispersion is forced by the freshwater outflow and by the tidal excursion at the offshore boundary. Unfortunately field data are not available for this condition, but only for different scenarios commented in the later sections.
Fig. 4A presents the results of a simulation carried out in the absence of coastal surface current and wind velocity lower than 1 knot. Simulation conditions are representative of the cycle of freshwater outfall in which tide, according with internal basin storage volumes, provides outgoing velocity from the channel mouth starting from 10.00 a.m. and ending 18 hours later at 4.00 a.m. The physical feature of the presented simulation is characterized by a first low decreasing tidal phase and low outgoing velocity typical of the last summer periods. The tidal excursion at several tidal phases is shown in Fig. 4B.

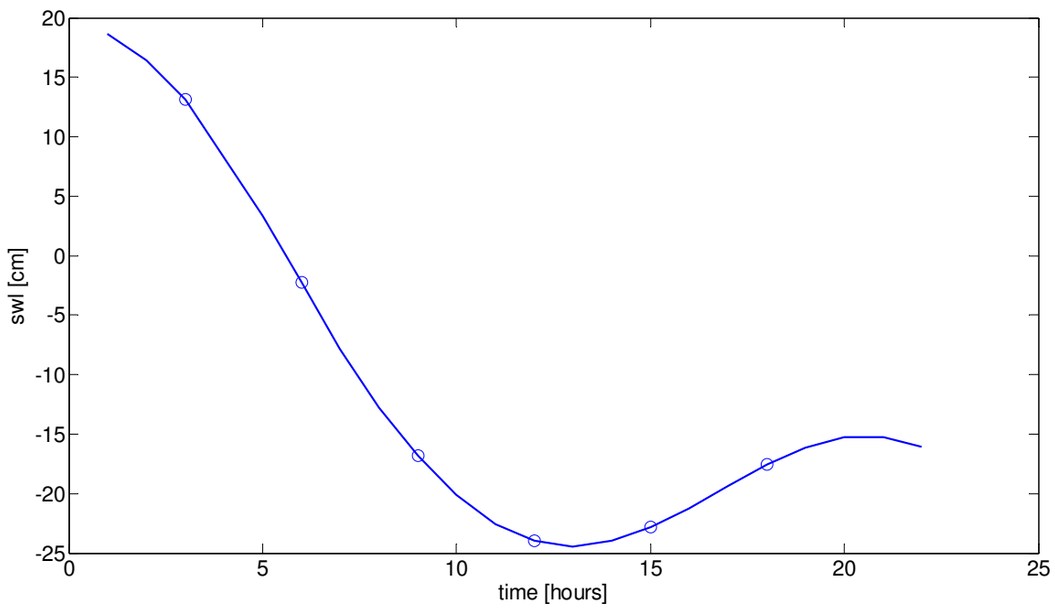


Fig. 4B. Sea water level at the offshore boundary during simulation with results in Fig. 3.

Here, in the early afternoon, variations in salinity and phytoplankton biomass are limited and restricted to the near mouth area and the surface thermoaline profile could be conditioned by wind coastal waves. Evening and nightly scenarios show static conditions for coastal sea with very low current and undefined direction, while the most part of freshwater accumulated in the internal basin is outfalled from the mouth according to the maximum tidal decreasing phase. Thermoaline stratification is guaranteed, such as in internal harbour section as in the receiver coastal sea. The simulation period shown in Fig. 4 (12h-15h-18h) covers the main decreasing tidal phase, when most freshwater, coming from WWTP and confined into the internal channel according with tidal phase, is completely discharged through the harbour canal. Evident stratification conditions are represented in coastal sea away from the breakwaters, such as in the north and south zones. The maximum decrease in sea salinity concentrations is evaluated in 7-8 g/l within the south breakwater confined shore area near the south embankment. In this zone, water volumes flowing through restricted breakwater mouths permit higher incoming surface velocity and low depth permits near the beach vertical mixing and a more homogeneous areal distribution.

The results also reveal different effects on plume areal dispersion and on thermoaline profiles between zones confined by continuous breakwaters (north shore) and by discontinuous breakwater (south shore). Comparing salinity vertical distribution in internal and external points of the north continue breakwaters, under a surface layer (50-60 cm) almost corresponding to breakwater submergence (Lamberti et al., 2005), differences in salinity and oxygen profiles become significant. Freshwater dispersion appears obstructed in the internal north confined area because continuous breakwaters produce a "wall effect" for incoming plume with mass exchange reduced for deep layers. Here, in the absence of north directed sea currents, flows are allowed only from north-south boundary mouths with vertical mixing limited to the surface layer.

## 5. Validation of model results with in situ measurement campaigns

In 2009 several field campaigns took place in order to observe the hydrodynamics at the outfall, to measure the velocities of the flow and the water quality parameters in order to validate the model. The measurements were performed with the support of a Bellingardo 550 motorboat utilizing a Geo-nav 6sun GPS system, a Navman 4431 ultrasonic transducer and an YSI556 multi-parameter probe. Morphologic, hydraulic and water quality measurements were executed into the transition estuary of the harbour canal and near the mouth. The dispersion area and profile distribution of freshwater outgoing from the harbour mouth and discharged in the coastal area was investigated and monitored. Experiments were carried out on June 2009 and September 2009. The surface currents were observed with the aim of drifters properly designed to follow the surface pollution and oil (Archetti, 2009). The drifters (Fig. 5) were equipped with a GPS to acquire the geographical position every 5 minutes and an IRIDIUM satellite system was used to send data to a server. Simultaneously, tide, waves, wind and rainfall conditions were collected.

Fig. 5. Lagrangian drifter in the sea during the experiment.

### 5.1 Experiment I: June 18, 2009.

The first experiment was carried out on June 18, 2009. The wave conditions were measured by the wave buoy located 5 nautical miles off the shore of Cesenatico (details on the wave position and data are available at http://www.arpa.emr.it/sim/?mare/boa). The significant

wave height $H_S$ was lower than 0.3 m for the whole day. The measured sea water level and wave conditions on the day of the experiment are plotted in Fig. 6A. The weather conditions were very mild, without wind and with ascending tide, so we had the opportunity to monitor a condition driven only by the tidal excursion. Figure 6B shows the swl during the experiment and the contemporary velocity and direction of the drifters launched 1 km offshore from the Cesenatico harbour canal.

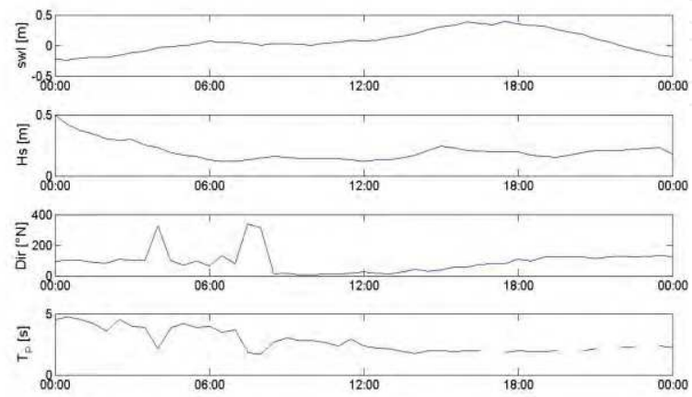


A

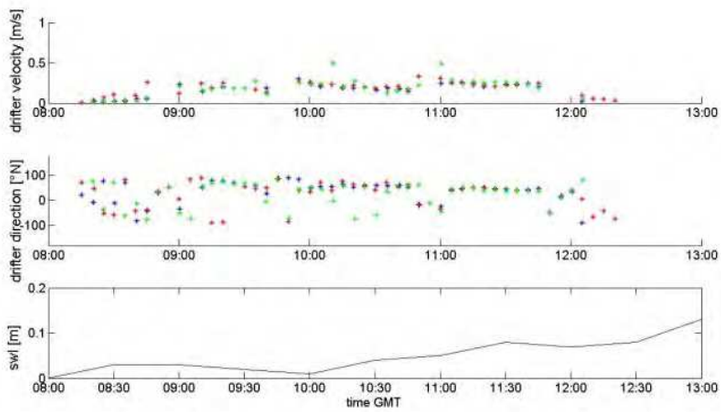


B

Fig. 6. A) Measured swl (top panel), significant wave height ($H_S$), direction and period ($T_P$). B), drifters' velocity (top panel), direction (central panel) and contemporary swl (bottom panel).

Clusters of three drifters were launched simultaneously at the offshore boundary. The launch position of the drifters is the offshore location in Fig. 7A. The first cluster was launched at about 9:00 a.m. just offshore from the harbour breakwaters, at a distance of 1.2 km from the beach, the second cluster was launched one hour later offshore from the northern beach and the last cluster was launched at 11:00 am offshore from the southern beach. The velocity and direction of the drifters during the experiment is plotted in Fig. 6B. The mean drifter velocity during the experiments was 0.18 m/s, with a direction perpendicular to the beach.


A

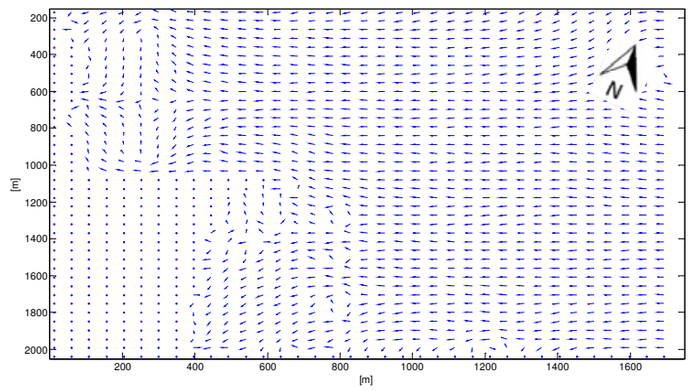


B

Fig. 7. A) Satellite view of the study area and pattern of two drifters launched on June 18, 2009. B). Field for experiment I of surface currents.

The observed condition was simulated by the model; the hydrodynamic was driven only by sea water tidal oscillation at the offshore boundary condition (condition in Fig. 6A ). The resulting surface current field during the experiment condition is shown in Fig. 7B, the current is perpendicular to the shoreline.
The field velocity appears comparable to the drifters' paths, both in direction and magnitude, so the model looks well calibrated.

### 5.2 Experiment II September 1, 2009

During the experiment carried out on September 1, 2009, the drifters were launched in the water in a plume of sewage water disposal from the canal of Cesenatico harbour. Two drifters were deployed in the plume centre and two at the plume front. The two drifters deployed at the plume front followed the plume front evolution during the experiment lasting 4 hours. Wind speed was approx. 30 m/s, significant wave height 0.5 m (Fig. 8A) and the tide descending. The plume and the drifters moved in the wind direction at an average speed of 0.2 m/s (Fig. 8B).

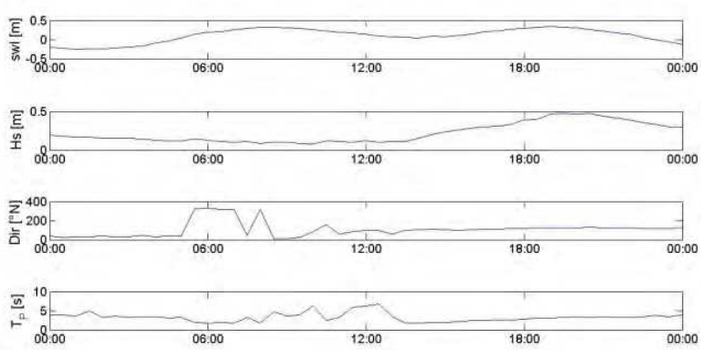


A

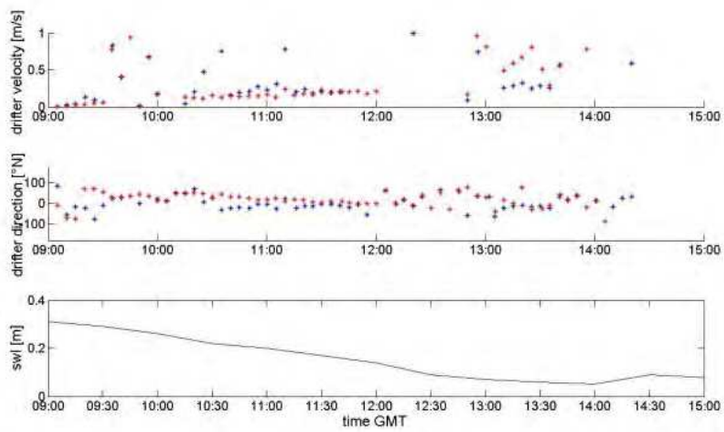


B

Fig. 8. A) Measured swl (top panel), significant wave height ($H_S$), direction and period ($T_P$). B) Drifters' velocity (top panel), direction (central panel) and contemporary swl (bottom panel).


A

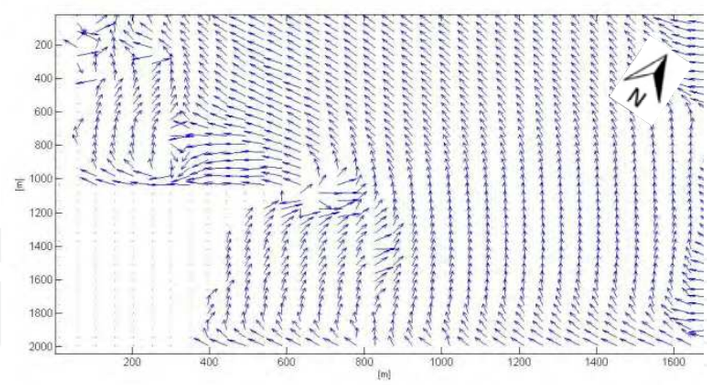


B

Fig. 9. A) Satellite view of the study area and pattern of three drifters launched on September 1, 2009. B). Surface currents' field for experiment II.

Differently from the previous examined condition, we observe here that the drifters' paths are north deviated by the action of the wind on the surface layer with higher velocity (Fig. 9A). The reorientation of the trajectory increases when the drifters approach the coast. Similar behaviour is observed in the hydrodynamic simulation results (Fig. 9B).
The observed and simulated effect is the result of the composition of the marine current driven by tidal oscillation, together with surface wind effect. The described condition is typical in summer in the final hours of the morning.
A model validation was also carried out by comparing simulated and observed salinity vertical profiles into the plume at section N3 during experiment II. The comparison (Fig. 10) shows a good agreement between observed and simulated values also in the vertical profiles. A more extensive comparison of vertical profiles with other parameters and at other sections will be performed in the future.

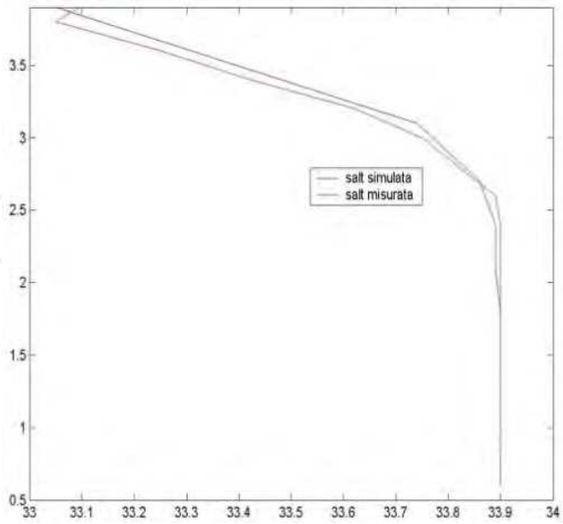


Fig. 10. Vertical salinity behaviour: observed in point N3 (red) and simulated by the model (blu).

During the experiments the presence of biological aggregates and foams was observed on the sea surface interested by the plume (Fig. 11). The presence of biological traces in sea areas interested by freshwater dispersion is a well known phenomenon. In a few cases bacterial and dead algae aggregate come directly from internal channels where variation in water depth provides alternance of photosynthetic and bacterial activity. Here, high aerobic biomass levels are produced by bacterial synthesis sustained by the production of photosynthetic oxygen of high growing algae populations. When oxygen, dissolved during light hours, cannot supply nightly bacteria/algal demand, the water column is interested by the presence of many species of died organic substances with the associated settling and floating phenomena. Production of biological foams can occur also when variations in salinity concentrations increase the mortality of a phytoplankton population growth in a low salinity environment. In these cases, foam presence is often registered in the last part of the harbour canal, near the sea mouth, and upon the plume boundary of the sea outfalled plume.

Two vertical profiles of temperature (Fig. 12A), dissolved oxygen, pH, (Fig. 12B) redox potential and salinity concentrations (Fig. 12A) were registered and analysed "on site" in order to check the main plume direction. Fixed investigated points are N1 and S1 focused as representing the north and south near the sea mouth area (see reference map in Fig. 2). Parameters are traced with reference to profile P6 at fixed points located on the east boundary in front of the harbour canal and chosen as indicators of offshore sea conditions.

No appreciable variations on salinity vertical distribution are registered in the south zone, where measured values appear very similar in S1 (south near mouth) and P6 (offshore sea). On the contrary, N1 vertical profile presents a salinity distribution which reveals the arrival in the surface layers of volumes coming from the mouth section enriched by internal freshwater. A difference of 2 g/l between bottom and surface layers with thermocline from depth of 60 to 120 cm is registered. Similarly, temperature does not show vertical variations in the south zone, even if media values appear lower in coastal rather than offshore sea water (26.5 °C) according with the cooling effects produced in September by internal water volumes. This is confirmed by the N1 temperature profile which presents lower values in surface layers (25.6°C) than in the underlying thermocline (26.4 °C) but inversion does not interrupt stratification which is maintained by variation in density. Similar temperature values in N1 and S1 points are registered within the thermocline thickness. At thermocline depths a temperature decrease is appreciable due to the colder masses stored at the bottom of the harbour canal.

N1, N2, N3 points, interested by the dispersion plume, show a pH vertical profile similar to temperature profile. Low pH values usually indicate biological organic substance degradation or nitrification phenomena typically active in waters of internal channels receiving wastewater. In N1 near the mouth point, higher values are confined in a 1 metre thickness layer, sited at a 1 metre depth. On this layer, lower pH values confirm the presence of a plume conditioned by freshwater also indicated by lower temperature.

Fig. 13 and Fig. 14 show the sequence of profiles obtained following the plume trajectory starting from P1 (internal point corresponding to the slipway) towards to N5 external point placed on the north boundary investigation area. As expected, freshwater volumes are progressively mixed with external high salinity volumes proceeding from internal to external sections. Vertical profiles of salinity behaviour at P1, P2, P3 internal points show that freshwater plume interests a 2 metre depth surface layer. At the last internal section (Gambero rosso), turbulence realizes a linear decrease on salinity concentration from 34 g/l

at 2 m depth to 31 g/l at the surface. This layer overflows upon an almost static high salinity volume placed at the bottom channel. Both P4 and N1 external profiles indicate clear stratification conditions with a 60 cm floating layer. Here, wastewater presence is appreciable and thermocline is located into the underlying 60 cm. Measured salinity surface values together with behaviour of vertical profiles allows the identification of an area interested by plume dispersion limited to a northerly direction by N3 fixed investigation point. Similar profiles at points N4 and N5 reveal that in experiment tidal and currents conditions are typical of offshore sea water volumes.

Fig. 11. View of the floating biological foams observed on the north plume boundary during the September 1, 2009 experiments. Photo taken from the N3 position (see Fig. 2) beach oriented.

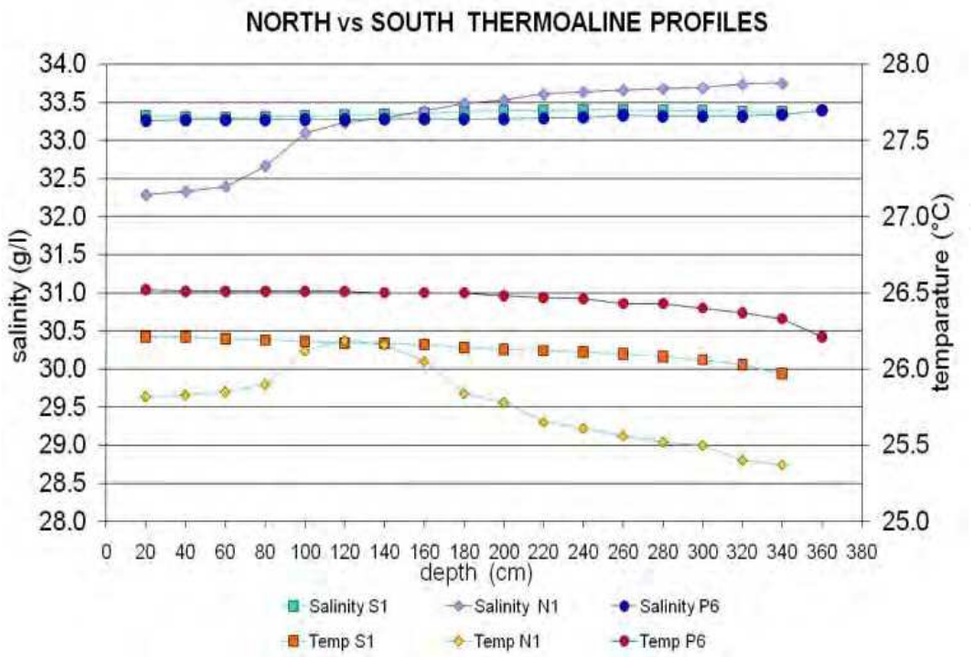


A

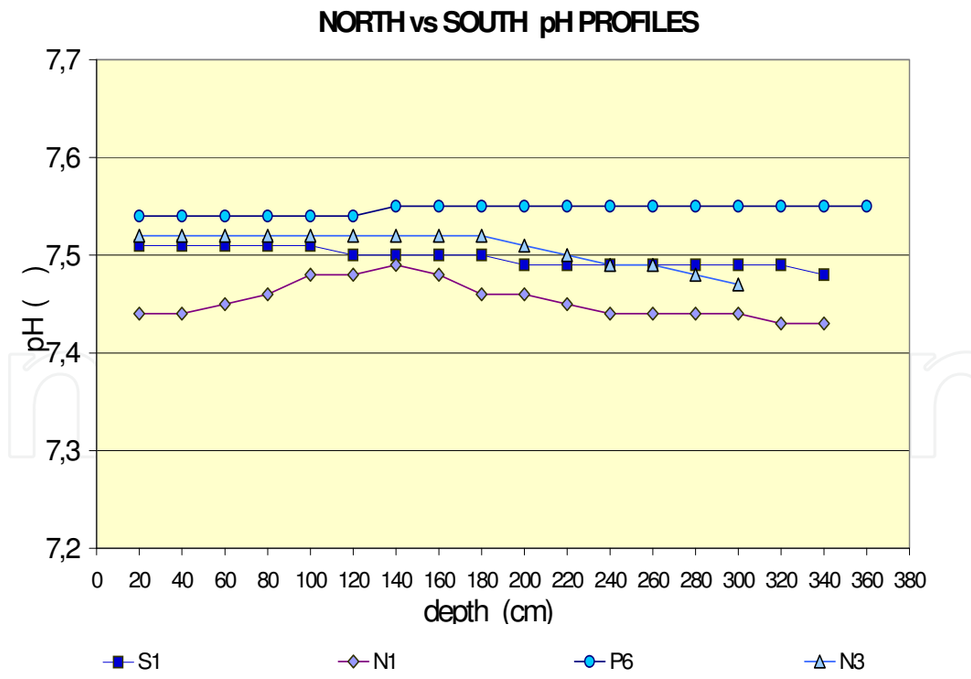


B

Fig. 12. A) Thermoaline and B) pH profiles at the beginning of the experiment at sections S1, N1, N3, P6 (see Fig.2).

The sequence of temperature profiles (Fig. 14) reveals very similar vertical trends and values among all profile sections inside the harbour canal (sections P1, P2 and P3). Perhaps a small effect of the external sea water's warmer mass could be noted in the deeper layers at P3 section sited in the proximity of the mouth. Excluding a 40cm sea bottom layer, all points' indicators of dispersion plume area present temperature values lower at surface (N1). As just reported in Fig. 12's comments on comparison of N1 and S1 thermoaline profiles, this initial thermal inversion which does not yet allow a stratification break, confirms salinity indications about plume areal extension. N5 profile, located at the northern boundary investigation area and not interested by colder freshwater coming from the internal basin, maintains a classic summer temperature profile for Adriatic coastal sea. In this case we observe a 26.4 °C constant temperature in a 120 cm depth surface layer, a thermocline to a depth of 240 cm and another 1 metre bottom layer with a constant temperature of 25.2 °C.

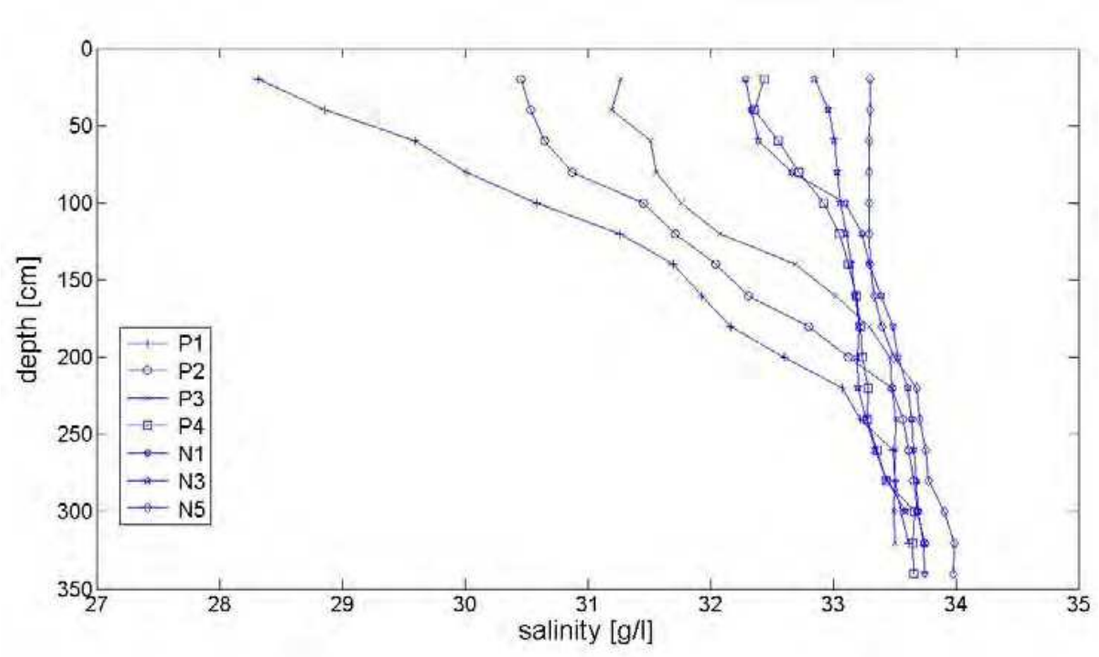


Fig. 13. Vertical profiles of salinity measured at the profile points during the experiment conducted on 1 September, 2009.

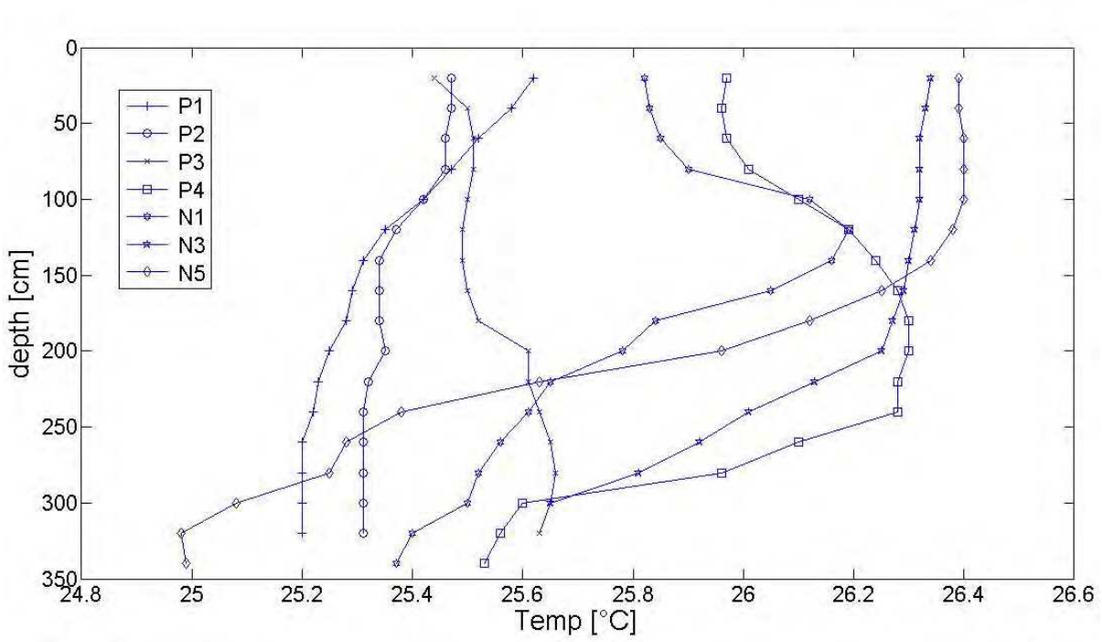


Fig. 14. Vertical profiles of temperature measured at the profile points during experiment conducted on 1 September, 2009.

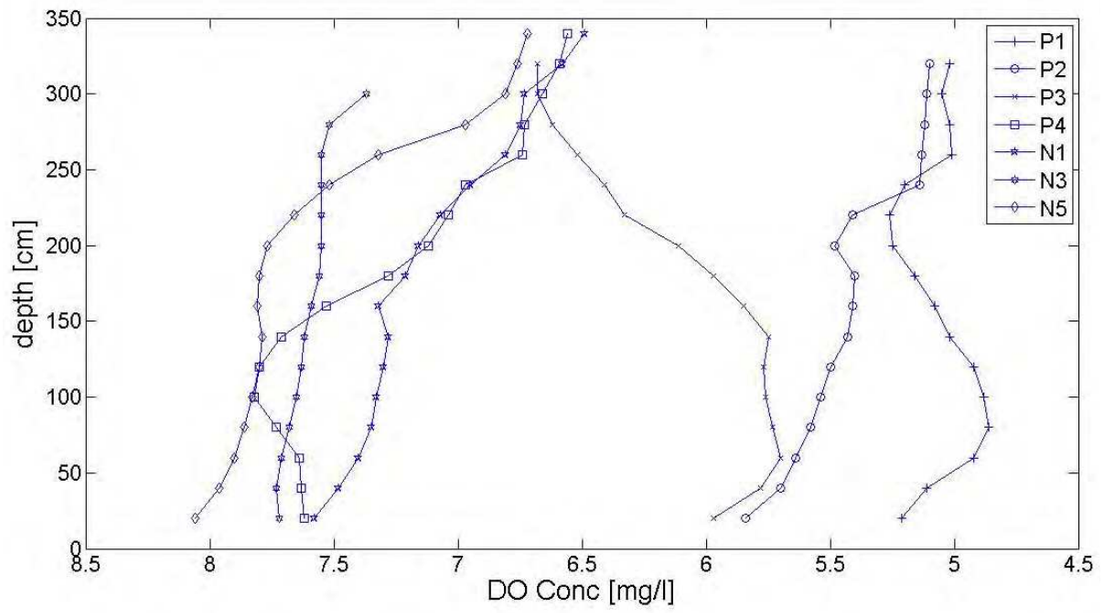


Fig. 15. Vertical profiles of dissolved oxygen at the profile points during experiment conducted on 1 September, 2009.

As expected, oxygen values averaged at each section (Fig. 15) increase, proceeding from internal to external points. At P1 and P2 profiles, photosynthesis produces maximum values in a 60 cm surface layer. At the P3 point (internal but near the mouth), a strong influence of external sea water on bottom layers is confirmed, which shows the same oxygen value, while at surface layers values are typical of internal waters. No information about plume dispersion could be obtained at external points where oxygen distribution is characterised by classic coastal sea profiles with oxygen decreasing values in the direction of deeper layers where photosynthesis is low and bacterial consumption increases.

Results of simulated salinity concentration (Fig. 16), similar to those presented in Fig. 4B, indicate a northerly oriented freshwater dispersion, different from the case analysed in Fig. 4B, which presents in the first phases a less oriented dispersion plume and during the following times (hour 15 – 18) a prevailing orientation to the southern coastal zone. In the actual case, the plume is west bounded by the continuous breakwaters, this means that the geometry is well reproduced in the model, and is dispersed to the north, for the effect of the wind, which was negligible in the previous examined condition.

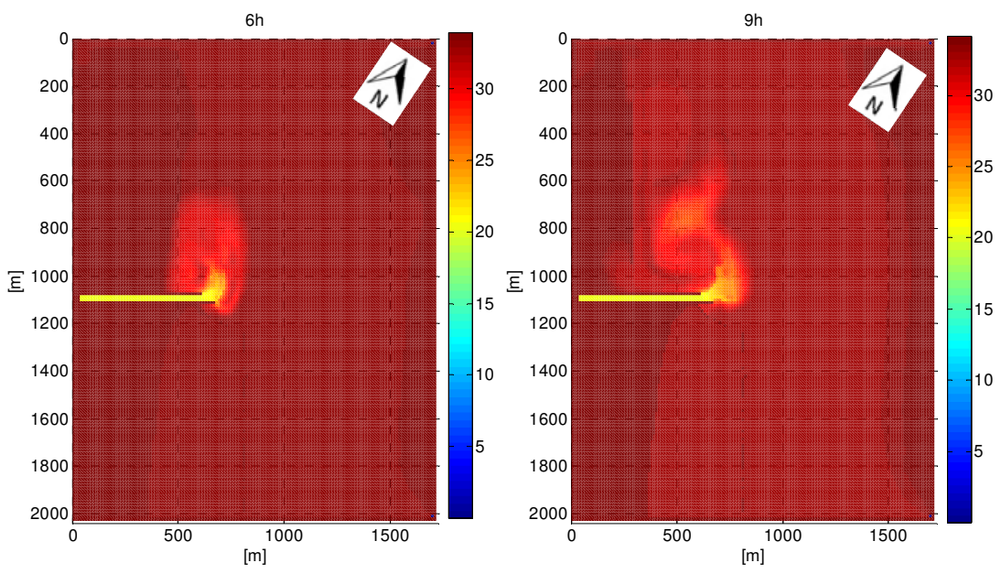


Fig. 16. Simulation of the freshwater plume dispersion during experiment II.

## 6. Conclusions

A freshwater dispersion plume in the sea has been described in depth in the present paper with the aim of producing a 3D numerical model and with the validation of two field campaigns carried out in different conditions. The investigated area concerns the coastal zone near Cesenatico (Adriatic Sea, Italy). The fresh water is dispersed by the canal harbour mouth into the open sea.

The model shows good performance in the application here presented, which is characterised by the presence of complex sea structures, requiring a very detailed and small mesh dimension in the geometry description.

Field data were acquired during two field campaigns and are of different typology: surface lagrangian paths, acquired by innovative properly designed drifters (in both campaigns); vertical profiles of temperature and salinity and dissolved oxygen acquired by a multiparameter probe in properly defined fixed points (in the second campaign). During the first campaign the hydrodynamic was driven only by the tidal oscillation and during the second also by surface wind, the tested conditions were therefore different and interesting for understanding the complex dynamics.

Comparison between model results and measurements are good for the surface hydrodynamic description and for the areal and vertical distribution of concentration, in particular, the resulting salinity values compared with experimental data have shown a surprisingly good agreement.

During the second experiment the presence of biological aggregates and foams was observed on the sea surface interested by the plume. The presence of biological traces in sea areas interested by freshwater dispersion is a well known phenomenon.

Vertical measurement of thermoaline parameters shows appreciable variations on salinity vertical distribution in the southern zone, where measured values appear very similar in the south near mouth and offshore sea. On the contrary, at the northern zone the vertical profiles present a salinitydistribution which reveals the arrival in the surface layers of volumes coming from the mouth section enriched by internal freshwater. A difference of 2 g/l between bottom and surface layers with thermocline from depth of 60 to 120 cm is registered. Similar behaviour was observed for temperature. In fact in the north the temperature profile presents lower values in surface layers (25.6°C) than in the underlying thermocline (26.4 °C), but inversion does not interrupt stratification which is maintained by variation in density. At thermocline depths a temperature decrease is appreciable due to the colder masses stored at the bottom of the harbour canal.

The points, interested by the dispersion plume, showed a pH vertical profile similar to temperature profile. Low pH values usually indicate biological organic substance degradation or nitrification phenomena typically active in waters of internal channels receiving wastewater. In N1 near the mouth point, higher values are confined in a 1 metre thickness layer, sited at a 1 metre depth. On this layer lower pH values confirm the presence of a plume conditioned by freshwater also indicated by a lower temperature.

The methodology proposed in this paper appears to be useful and accurate enough to simulate the dynamics of the freshwater dispersion at the investigated scale.

The results here presented are original and have allowed a general comprehension of the thermoaline and hydrodynamic assessment of the dispersion area.

The model now validated can in the future be applied to investigate the dispersion in other meteo climatic conditions, tides and other canal mouth geometries.

## 7. Acknowledgements

Authors are grateful to CIRI Edilizia e Costruzioni, UO Fluidodinamica for the financial support.

## 8. References

Archetti R. (2009). Design of surface drifter for the oil spill monitoring. *REVUE PARALIA. Coastal and Maritime Mediterranean Conference*. Hammamet, Tunisie (2009). 2-5 Dec. 2009. vol. 1, pp. 231 - 234 http://www.paralia.fr/cmcm/hammamet-2009.htm.

Bragadin G.L., Mancini M.L., Turchetto A. (2009). Wastewater discharge by estuarine transition flow and thermoaline conditioning in shore habitat near Cesenatico breakwaters. *Proceeding of the Fifth International Conference on Coastal Structures. Coastal Structures 2007*-Venice.July 2-4, 2007 (vol.II, pp.1101-1112).

Broche P. Devenon J.L., Forget P., Maistre C., Naudin J. and Cauwet G. (1998). Experimental study of the Rhone plume. Part I. Physics and dynamics. *Oceanol Acta. 21, 725-738. ISSN: 0399-1784.*

Burrage D., J. Wesson, C. Martinez, T. Pérez, O. Möller Jr., A. Piola. (2008). Patos Lagoon outflow within the Río de la Plata plume using an airborne salinity mapper: Observing an embedded plume. *Continental Shelf Research*, 28 (13), 1625-1638. ISSN: 0278-4343.

Di Giacomo P. M., Washburn L., Holt B. and Jones B. H. (2004). Coastal pollution hazards in southern California observed by SAR imagery: stormwater plumes, wastewater plumes and natural hydrocarbon seeps. *Marine Pollution Bulletin* 49 (2004) 1013–1024. ISSN 0025-326X.

Duran N., Fiandrino A., Frauniè P., Ouillon S., Forget P. and Naudin J. (2002). Suspended matter dispersion in the Ebro ROFI: an integrated approach. *Continental Shelf Research* 22, 267-284. ISSN 0278-4343.

Fichez R., Jickells T. D. and Edmunds H. M. (1992). Algal blooms in high turbidity, a result of the conflicting consequences of turbulence on nutrient cycling in a shallow water estuary. *Estuary Coast Shelf Sci*. 35. 577 – 593. ISSN 0272-7714.

Figueiredo da Silva F., Duck R.W., Hopkins T.S. and Anderson J.M. (2002). Nearshore circulation revealed by wastewater discharge from a submarine outfall, Aveiro Coast, Portugal. *Hydrology and Earth System Sciences* 6(6), 983–989 (2002). ISSN: 1027-5606.

Froidefond J.M., Jegou A.M., Hermida J., Lazure P., Castaing P. (1998). Variability of the Gironde turbid plume by remote sensing. Effect of climate factor. *Oceanol Acta*. 21: 191-207. ISSN: 0399-1784.

Garvine R.W. (1987). Estuarine plumes and fronts in shelf waters: a layer model. *Journal of Physical Oceanography* 17 (1987), 1877–1896. ISSN: 0022-3670.

Garvine, R.W. (1995). A dynamical system for classifying buoyant coastal discharges. *Continental Shelf Research* 15 (13) (1995), pp. 1585–1596. ISSN: 0278-4343.

Grimes C. and Kingford M. (1996). How do riverine plumes of different sizes influence fish larvae: do they enhance recruitment? *Marine Freshwater Research*. 47, 191-208. ISSN: 1323-1650.

Jouanneau J. M. and Latouche C. (1982). Estimation of fluxes to the ocean from mega tidal estuaries under moderate climates and the problems they present. *Hydrobiologia*, 91. 23:29. ISSN: 0018-8158.

Kourafalou V.H., Lee T.N., Oey L.-Y. and Wang J.D. (1996). The fate of river discharge on the continental shelf, 2. Transport of coastal low-salinity waters under realistic wind and tidal forcing. *Journal of Geophysical Research* 101 (1996), 3435–3455. ISSN 0148-0227.

Lamberti A., Archetti R., Kramer M., Paphitis D., Mosso C., Di Risio M. (2005). European experience of low crested structures for coastal management. *Coastal Engineering*. Vol. 52.(10-11), 841 - 866 ISSN 0378-3839.

Liu S.K. and Leendertse J.J. (1978). Multidimensional numerical modelling of estuaries and coastal seas, *Advances in Hydroscience*, Vol. 11, Academic Press, New York (USA), 1978. ISSN: 0065-2768.

Mestres M., Sierra J.P., Sánchez-Arcilla A. (2007). Factors influencing the spreading of a low-discharge river plume. *Continental Shelf Research*, 27, (16-15), 2116-2134. ISSN: 0278-4343.

Mancini M.L. (2008). Wastewater finishing by combined algal and bacterial biomass in a tidal flow channel. Modeling and field experiences in Cesenatico. *International Symposium on Sanitary and Environmental Engineering-SIDISA 08 -Proceedings, ROMA, ANDIS*, 2008, pp. 50/1 - 50/8

Mancini M.L. (2009). Wastewater discharge and thermoaline conditioning in south Cesenatico (I) coastal area near breakwaters. *Proceedings of the Ninth International Conference on the Mediterranean Coastal Environment.-MEDCOAST 09.* Sochi-Russia. 10-14 November 2009. vol. 1, 143/1 - 143/7.

Mestres M., Sierra J.P., Sanchez Arcilla, A., Del Rio, J.G., Wolf T., Rodriguez A. and Ouillon S. (2003). Modelling of the Ebro River plume. Validation with field observations. *Scientia Marina*. 67 (4). 379 – 391. ISSN 0214-8358.

Molleri G. S. F., De M. Novo E. M. L., Kampel M. (2010). Space-time variability of the Amazon River plume based on satellite ocean color. Continental Shelf Research 30 (3-4). 342-352. ISSN: 0278-4343.

Nezlin G.P and DiGiacomo P.M. Satellite ocean color observations of stormwater runoff plumes along the San Pedro Shelf (southern California) during 1997–2003. (2005). *Continental Shelf Research*, 25,(14), 1692-1711. ISSN: 0278-4343.

Ogston A. S., Cacchione D. A., Sternberg R. W., Kineke G. C. (2000). Observations of storm and river flood-driven sediment transport on the northern California continental shelf. *Continental Shelf Research*, 20, (16), 2141-2162.

O'Donnell J. (1990). The formation and fate of a river plume: a numerical model. *J. Phys. Oceanogr*. 20, 551-569. ISSN: 1520-0485.

Sherwin T. J., Jonas P. J. C. and Sharp C. Subduction and dispersion of a buoyant effluent plume in a stratified English bay. *Marine Pollution Bulletin*, Vol. 34, No. 10, 827-839, 1997. ISSN 0025-326X.

Siegel H., Gerth M. and Mutze A. (1999). Dynamics of the Oder River plume in the southern Baltic Sea: Satellite data and numerical modelling. *Continental Shelf Research* 19 (1143 – 1159). ISSN: 0278-4343.

Stumpf R.P., Gefelbaum G. and Pennock J.R. (1993). Wind and tidal forcing of a buoyant plume, Mobile Bay, Alabama. *Continental Shelf Research* 13, 1281-1301. ISSN: 0278-4343.

Yankovsky E. and Chapman D.C. (1997). A simple theory for the fate of buoyant coastal discharges. *Journal of Physical Oceanography* 27 (1997), 1386–1401 ISSN: 1520-0485.

Warrick J. A. and Stevens A. W. (2011). A buoyant plume adjacent to a headland—observations of the Elwha River plume. *Continental Shelf Research*, 31,85-97. ISSN: 0278-4343.

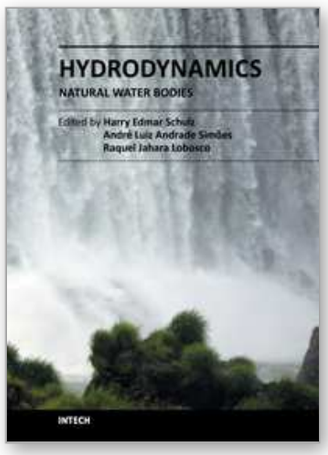


**Hydrodynamics - Natural Water Bodies**
Edited by Prof. Harry Schulz

ISBN 978-953-307-893-9
Hard cover, 286 pages
**Publisher** InTech
**Published online** 05, January, 2012
**Published in print edition** January, 2012

The knowledge of the characteristics of the fluids and their ability to transport substances and physical properties is relevant for us. However, the quantification of the movements of fluids is a complex task, and when considering natural flows, occurring in large scales (rivers, lakes, oceans), this complexity is evidenced. This book presents conclusions about different aspects of flows in natural water bodies, such as the evolution of plumes, the transport of sediments, air-water mixtures, among others. It contains thirteen chapters, organized in four sections: Tidal and Wave Dynamics: Rivers, Lakes and Reservoirs, Tidal and Wave Dynamics: Seas and Oceans, Tidal and Wave Dynamics: Estuaries and Bays, and Multiphase Phenomena: Air-Water Flows and Sediments. The chapters present conceptual arguments, experimental and numerical results, showing practical applications of the methods and tools of Hydrodynamics.



**InTech Europe**
University Campus STeP Ri
Slavka Krautzeka 83/A
51000 Rijeka, Croatia
Phone: +385 (51) 770 447
Fax: +385 (51) 686 166
www.intechopen.com

**InTech China**
Unit 405, Office Block, Hotel Equatorial Shanghai
No.65, Yan An Road (West), Shanghai, 200040, China
中国上海市延安西路65号上海国际贵都大饭店办公楼405单元
Phone: +86-21-62489820
Fax: +86-21-62489821

IntechOpen